Journal of Statistical Physics, Vol. 94, Nos. 5/6, 1999

Multifractal Statistics of Mesoscopic Systems

A. Bershadskii[1]

Received May 7, 1998; final September 17, 1998

A generalization of the Havlin–Bunde multifractal hypothesis is used to obtain a probability distribution corresponding to mesoscopic systems close to the critical regime. Good agreement between results of numerical simulations performed by different authors and this new type of probability distribution is established.

KEY WORDS: Multifractal Bernoulli distribution; disordered systems.

1. INTRODUCTION

In mesoscopic regime (i.e., for phase coherent systems) and in presence of disorder the electronic states can become localized. Such a system can exhibit a transition from localized to extend eigenstates. Moreover, close to the transition the wave functions fluctuate on all scales up to the system size L and the squared modulus of these critical wave functions forms a multifractal measure (see, for instance, ref. 1 and references therein). Multifractality is an indication for broad distributions of scaling variables. To find an universal probability distribution corresponding to this situation (if such distribution exists) is an actual problem.

The generalized fractal dimensions—D_q, are generally used to describe the multifractal regimes. For small q, for instance, linear approximation of D_q corresponds to the log-normal distribution.[1, 2] The linear approximation is generally applicable in a narrow vicinity of point $q=0$ only. Thus, one should seek an adequate representation for D_q (different from the "log-normal") behind of this vicinity. While the log-normal distribution has an universal character (corresponding to the linear approximation of D_q in a vicinity of point $q=0$) this new statistical distribution should have more

[1] P.O. Box 39953, Ramat-Aviv 61398, Tel-Aviv, Israel.

0022-4715/99/0300-0725$16.00/0

special nature and should correspond to the transition from monofractality[3] to multifractality.

In the present paper a new method to obtain such statistical distribution is suggested. This method based on a generalization of the Havlin–Bunde multifractal hypothesis.[4] Characteristic function of this probability distribution has been obtained in an explicit form. It is shown that this distribution corresponds to some multifractal generalization of the Bernoulli distribution. A representation of the generalized dimensions D_q, corresponding to the multifractal Bernoulli distribution, has been compared with results of numerical calculations performed by different authors for different models of the mesoscopic systems.[5–8]

The localization properties of the eigenstates are also reflected in the spectral properties of the systems. It is shown in ref. 5 (see also ref. 9) that there is a simple relationship between the generalized dimensions constructed on spatial and on spectral measures. In the present paper we apply the multifractal Bernoulli distribution also to data obtained in ref. 10 for eigenstates spectrum of a quasi-periodically driven (kicked) spin system. The kicked quantum systems give also another remarkable example of applicability of the multifractal Bernoulli distribution. Namely, the kicked rotator (quantized standard map) exhibits dynamical localization that bears analogies with Anderson localization in 1D lattices.[11] The multifractal analysis of the spectral measure of the Kicked Harper Model performed in ref. 11 allows to apply the multifractal Bernoulli distribution to such class of multifractal systems as well.

2. MULTIFRACTAL BERNOULLI DISTRIBUTION

A continuous set of the exponents, so-called generalized dimensions—D_q is usually used to described the multifractal behavior. These generalized dimensions are determined from equation

$$Z(q) = \sum_{i=1}^{N} [\,\mu_i(r)\,]^q \sim (r/L)^{\tau(q)} \tag{1}$$

where

$$\tau(q) = (q-1)\, D_q \tag{2}$$

and given lattice with linear system size L is partitioned into N boxes of size r ($N \sim (L/r)^d$, d is the topological dimension of the lattice), the measure μ_i is the amplitude of the wave function squared on the ith box and the limit $r/L \to 0$ is taken.

Let us define

$$\overline{\mu_i} = \mu_i / \max_i \{\mu_i\} \tag{3}$$

Then

$$\langle \bar{\mu}^p \rangle = \frac{1}{N} \sum_i \overline{\mu_i}^p \tag{4}$$

A simplest structure, that can be used for fractal description, is a system for which $\overline{\mu_i}$ can take only two values 0 and 1. It follows from (3) and (4) that for such system (with $p > 0$)

$$\langle \bar{\mu}^p \rangle = \langle \bar{\mu} \rangle \tag{5}$$

and fluctuations in this system can be identified as Bernoulli fluctuations.[12] It is clear that the Bernoulli fluctuations can be *monofractal* only.

Generalization of (5) in form of a generalized scaling

$$\langle \bar{\mu}^p \rangle \sim \langle \bar{\mu} \rangle^{f(p)} \tag{6}$$

can be used to describe more complex (multifractal) systems. We use invariance of the generalized scaling (6) with dimension transform[13]

$$\overline{\mu_i} \to \overline{\mu_i}^{\lambda} \tag{7}$$

to find $f(p)$. This invariance means that

$$\langle (\bar{\mu}^{\lambda})^p \rangle \sim \langle (\bar{\mu}^{\lambda}) \rangle^{f(p)} \tag{8}$$

for all positive λ. Then, it follows from (6) and (8) that

$$\langle (\bar{\mu})^{\lambda p} \rangle \sim \langle \bar{\mu} \rangle^{f(\lambda p)} \sim \langle \bar{\mu} \rangle^{f(\lambda)\, f(p)} \tag{9}$$

Hence,

$$f(\lambda p) = f(\lambda)\, f(p) \tag{10}$$

General solution of functional equation (10) is

$$f(p) = p^{\gamma} \tag{11}$$

where γ is a positive number. This relationship can be considered as a generalization of the Havlin–Bunde multifractal hypothesis.[4] It should be

noted that case $\gamma = 1$ corresponds to Gauss fluctuations.[14] We, however, shall consider limit $\gamma \to 0$ (i.e., transition to the Bernoulli fluctuations). This transition is non-trivial. Indeed, let us consider generalized scaling

$$F_{qm} \sim F_{km}^{\alpha(q,k,m)} \tag{12}$$

where

$$F_{qm} = \langle \bar{\mu}^q \rangle / \langle \bar{\mu}^m \rangle \tag{13}$$

Substituting (6) into (12), (13) and using (11) we obtain

$$\alpha(q,k,m) = \frac{q^\gamma - m^\gamma}{k^\gamma - m^\gamma}$$

Hence,

$$\lim_{\gamma \to 0} \alpha(q,k,m) = \frac{\ln(q/m)}{\ln(k/m)} \tag{14}$$

If there is ordinary scaling

$$\langle \bar{\mu}^p \rangle \sim (r/L)^{\zeta_p} \tag{15}$$

then

$$\alpha(q,k,m) = \frac{\zeta_q - \zeta_m}{\zeta_k - \zeta_m} \tag{16}$$

From comparison (14) and (16) we obtain at the limit $\gamma \to 0$

$$\frac{\zeta_q - \zeta_m}{\zeta_k - \zeta_m} = \frac{\ln(q/m)}{\ln(k/m)} \tag{17}$$

General solution of functional equation (17) is

$$\zeta_q = a + c \ln q \tag{18}$$

where a and c are some constants.

If we use relationship

$$\max_i \{\mu_i\} \sim (r/L)^{D_\infty} \tag{19}$$

(see, for instance, ref. 15), then it follows from (2), (3) and (15), (18), (19) that

$$D_q = D_\infty + c\,\frac{\ln q}{(q-1)} \tag{20}$$

for the multifractal Bernoulli fluctuations (i.e., for the fluctuations which appear at the limit $\gamma \to 0$).

From (6), (15) and (18) we can find $f(p)$ corresponding to the multifractal Bernoulli fluctuations

$$f(p) = 1 + \frac{c}{a}\ln p \tag{21}$$

where $a = d - D_\infty$. One can see that for finite c the dimension-invariance is broken at the limit $\gamma \to 0$.

Let us find the characteristic function of the multifractal Bernoulli distribution. It is known that the characteristic function $\chi(\lambda)$ can be represented by following series (see, for instance ref. 12)

$$\chi(\lambda) = \sum_{p=0}^{\infty} \frac{(i\lambda)^p}{p!} \langle \bar{\mu}^p \rangle \tag{22}$$

Then using (6) and (21) we obtain from (22)

$$\chi(\lambda) = 1 + \langle \bar{\mu} \rangle \sum_{p=1}^{\infty} \frac{(i\lambda)^p}{p!}\, p^\beta \tag{23}$$

where

$$\beta = \frac{c}{(d - D_\infty)} \ln \langle \bar{\mu} \rangle \tag{24}$$

The characteristic function (23) gives complete description of the multifractal Bernoulli distribution. When $c = 0$ distribution (23)–(24) coincides with the simple Bernoulli distribution.[12]

It follows from (3) and (4) that $\langle \bar{\mu} \rangle \leqslant 1$. Therefore one obtains from (24) that $\beta \leqslant 0$ (due to $\ln \langle \bar{\mu} \rangle \leqslant 0$, $0 \leqslant c$, and $0 \leqslant d - D_\infty$). This is significant because for $\beta > 0$ the representation (23) may not correspond to a normalized probability. Indeed, for this characteristic function $\langle \bar{\mu}^p \rangle = \langle \bar{\mu} \rangle\, p^\beta$. On the other hand, by Hölder inequality one has

$$\langle \bar{\mu}^p \rangle \leqslant \langle \bar{\mu}^{pq} \rangle^{1/q}$$

for any integer q. Therefore

$$\langle \bar{\mu} \rangle p^{\beta} \leqslant \langle \bar{\mu} \rangle^{1/q} (pq)^{\beta/q}$$

Letting q tend to infinity in the above inequality one obtains

$$\langle \bar{\mu} \rangle p^{\beta} \leqslant 1$$

Since $\langle \bar{\mu} \rangle \leqslant 1$ and $1 \leqslant p$ (in representation (23)), then this inequality is satisfied for $\beta \leqslant 0$ and it is not satisfied (for large enough p) when $\beta > 0$. Therefore the characteristic function (23) corresponds to some real probability distribution for $\beta \leqslant 0$ only (that takes place in our case (24)).

The multifractality–monofractality phase transition (with $\gamma \to 0$) corresponds to a gap from $c = 0$ to a finite non-zero value of c. If we use a thermodynamic interpretation of the multifractality represented in ref. 16, then the constant c can be interpreted as multifractal specific heat of the system. The gap of the multifractal specific heat at the multifractality–monofractality transition (i.e., with $\gamma \to 0$) allows us consider this transition as a thermodynamic phase transition.[17]

3. CRITICAL MESOSCOPIC SYSTEMS: EIGENSTATES

In a recent paper[5] numerical calculations of the local density states at disorder-induced localization–delocalization transitions were performed for two- and three-dimensional network models of the integer quantum Hall effect[18] and the so-called quantum Hall insulator, respectively. Figure 1 (adapted from ref. 5) shows the function $D_q/2$ calculated for a two-dimensional network model at the quantum Hall critical point.[18, 19] In this figure the axes are chosen for comparison between the data (dots) and the multifractal Bernoulli representation (20) (straight line). One can see good agreement between the data and the representation (20). Figure 2 (also adapted from ref. 5) shows the analogous data calculated in ref. 5 for a three-dimensional network.[20] In contrast to the two-dimensional network, here a band of extended states appears. And again, the multifractal Bernoulli fluctuations appear at the mobility edge of this system, as one can see from Fig. 2 (in Fig. 2 straight line corresponds to the multifractal Bernoulli representation (20)). In ref. 6 the authors have examined the three-dimensional Schrödinger equation with a random potential at each lattice site, described by the Anderson Hamiltonian:

$$H = \sum_{\mathbf{x}} \varepsilon_{\mathbf{x}} |\mathbf{x}\rangle\langle \mathbf{x}| + V \sum_{(\mathbf{x}, \mathbf{y})} |\mathbf{x}\rangle\langle \mathbf{y}|$$

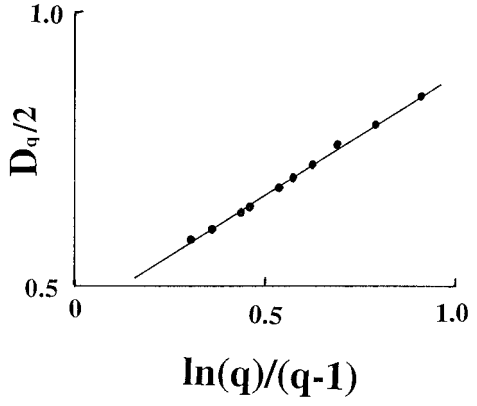

Fig. 1. Generalized dimensions $D_q/2$ against $\ln(q)/(q-1)$ for a 2D network model at the quantum Hall critical point. Data (dots) taken from ref. 5. The straight line is drawn for comparison with representation (20).

with constant nearest-neighbor transfer integral V and random potential $\varepsilon_{\mathbf{x}}$ governed by an uniform distribution of width W. The sums extend over all lattice sites $\mathbf{x}$ and $(\mathbf{x}, \mathbf{y})$ denotes all nearest-neighbor pairs of sites in a three-dimensional lattice. The parameter W describes the strength disorder and the metallic-insulator transition is believed to occur at $W_c \simeq 16.5$ for 3D samples.[21, 22] For $W > W_c$ all states are localized and the conductivity is zero, while for $W < W_c$ mobility edges appear in the band separating localized states near the band centre. In ref. 6 the model equation was

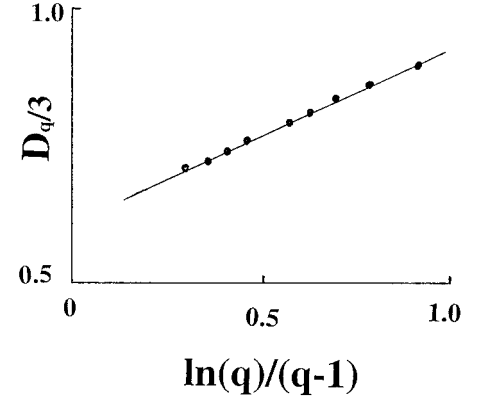

Fig. 2. Generalized dimensions $D_q/3$ against $\ln(q)/(q-1)$ for a 3D network model. Data (dots) taken from ref. 5. The straight line is drawn for comparison with representation (20).

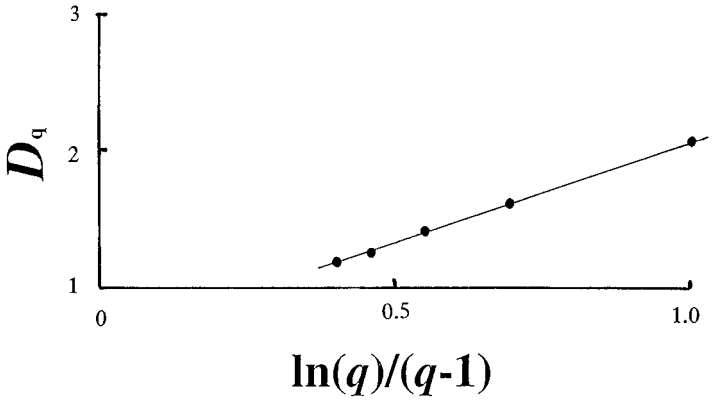

Fig. 3. Generalized dimensions D_q against $\ln(q)/(q-1)$ for 3D Anderson transition. Data (dots) taken from ref. 6. The straight line is drawn for comparison with representation (20).

numerically studied at the critical region and the generalized dimensions D_q were calculated by plotting $\ln(\langle \sum_{\mathbf{x}} |\psi_n(\mathbf{x})|^{2q} \rangle)$ against $\ln(L)$. These data (taken from ref. 6) are shown in Fig. 3. The axes on this figure are chosen for comparison with representation (20) (straight line). One can see good agreement between the data (dots) and this representation. In ref. 7 analogous multifractal spectrum was calculated for eigenstates in the critical regime of a two dimensional electron gas in high magnetic field. Figure 4 (adapted from ref. 7) shows these data. One can see good agreement between the data (dots) and the Bernoulli representation (20).

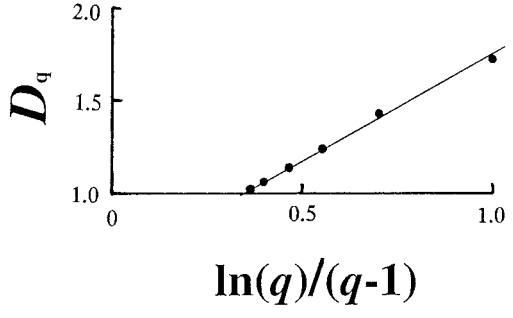

Fig. 4. Generalized dimensions D_q against $\ln(q)/(q-1)$ for multifractal wavefunctions in the critical regime of 2D disordered electron systems in high magnetic field. Data (dots) taken from ref. 7. The straight line is drawn for comparison with representation (20).

4. ANDERSON TRANSITION IN SYSTEMS WITH LONG-RANGE DISORDER

From the previous section we can suppose that the multifractality–monofractality phase transition takes place in a vicinity of the Anderson phase transition. Now the question is: Whether the multifractality–monofractality phase transition takes also place in the Anderson model with long-range disorder. For the long-range off-diagonal 3D disorder where the nondiagonal matrix elements $V(R)$ falling off $\propto 1/R^3$ or slower all states are delocalized[23, 24] (on other dimensions, d, this result can be extended replacing $1/R^3$ by $1/R^d$). This dependence of transition matrix elements is characteristic for the dipole interaction between elastic defects in solids. Such type of interaction between soft harmonic oscillators leads to universal linear frequency dependence of the density of states above the boson peak in glasses.[25] Because of the long-range correlations these delocalized states have multifractal spatial structure causing anomalous diffusion of excitation in the system.

In a recent paper[8] a numerical simulation of such type of a system was performed. Off-diagonal disorder was introduced as $V_{ij} = (\pm 1)/|\mathbf{R_i} - \mathbf{R_j}|^d$. Here R_i are Poisson-distributed random points in d dimensional space, and the random sign, ± 1 provides for the average value $\langle V_{ij} \rangle = 0$ corresponding

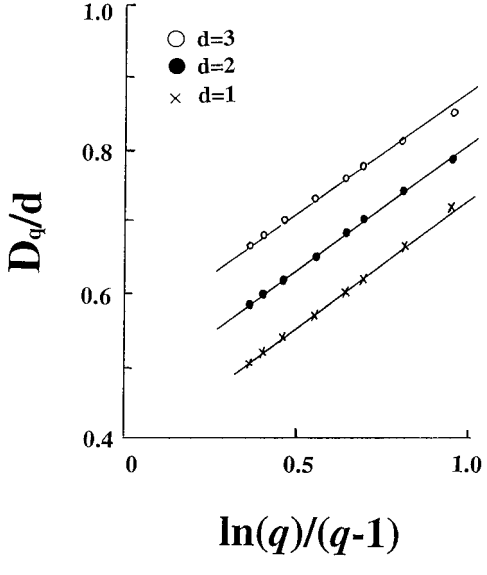

Fig. 5. Generalized dimensions D_q/d against $\ln(q)/(q-1)$ for the most extended eigenstates. Data (symbols) taken from ref. 8. The straight lines are drawn for comparison with multifractal Bernoulli's representation (20).

to the interaction of randomly oriented electric or elastic dipoles. Figure 5 (adapted from ref. 8) shows generalized dimensions spectra obtained in this numerical simulation for the most extended eigenstates in the spaces with different dimensions: $d=1,\ 2,\ 3$. The straight lines are drawn for comparison with the multifractal Bernoulli representation (20). One can also calculate $c \simeq d/3$ from this figure. It is interesting to compare this relationship with relationship $c=d/2$ corresponding to the case of the ideal monoatomic gas (where this relationship has purely geometrical nature related to space dimensionality[17]). To obtain the relationship $c=d/3$ for the multifractal thermodynamics of the Anderson model with long-range disorder from generalized geometrical arguments seems to be an interesting problem for future investigations.

5. MULTIFRACTAL BERNOULLI DISTRIBUTION OF EIGENVALUES

The localization properties of the eigenstates are also reflected in the spectral properties of the system. For such systems the spectral measure excited by a wave packet is multifractal. In particular, it was found in ref. 9 that enhanced return probability of wave packets at the mobility edge of quantum Hall systems could be interpreted both from the spectral as well as the spatial properties of the local density states. Then it is shown in ref. 5 that at the mobility edge the generalized dimensions corresponding to the spatial and spectral descriptions are proportional with a coefficient equal to the space dimensions of the system. The data shown in Figs. 1 and 2 are obtained in ref. 5 both from spatial and spectral analysis of the systems. The generalized dimensions obtained in ref. 5 by both the methods agree within the errors estimation.

Figure 6 (adapted from ref. 10) shows the generalized dimensions spectrum D_q for multifractal data (dots) obtained in a recent numerical simulation of a quasi-periodically driven (kicked) spin-$\frac{1}{2}$ system with singular continuous spectrum. One can see that these data (constructed on the spectral measure) is in good agreement with the Bernoulli representation (20) (straight line).

The kicked quantum systems give also another remarkable example of spectrum with multifractal measure. The kicked rotator (quantized standard map) exhibits dynamical localization that bears analogies with Anderson localization in 1D lattices.[11, 26] The Kicked Harper Model is obtained upon quantization of the following area-preserving map[11]

$$p_{n+1}=p_n+K\sin(x_n), \qquad x_{n+1}=x_n-L\sin(p_{n+1})$$

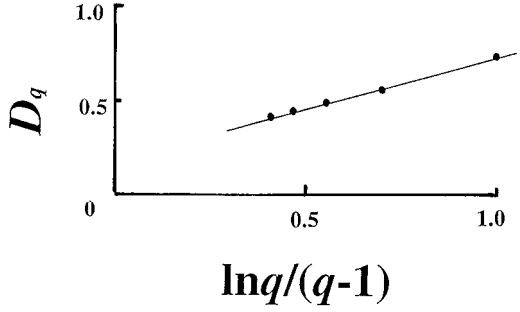

Fig. 6. Generalized dimensions D_q for a quasi-periodically driven (kicked) spin-$\frac{1}{2}$ (results of numerical simulation performed in ref. 10). The solid straight line indicates agreement of these data with the Bernoulli representation (20).

Canonical quantization thus leads to the one period evolution operator

$$U = \exp\left\{-i\,\frac{L}{h}\cos(h\hat{n})\right\}\exp\left\{-i\,\frac{K}{h}\cos(x)\right\}$$

where $\hat{n} = -i\,\partial/\partial x$, and $h/2\pi$ has to be considered as effective Planck constant, playing a role similar to an incommensurability parameter in a quasi-periodic system. A multifractal analysis performed for this model in ref. 11 gives a set of generalized dimensions constructed on spectral measure of this system. Figure 7 (adapted from ref. 11) shows these generalized dimensions for two values of dimensionless time—400 (lower

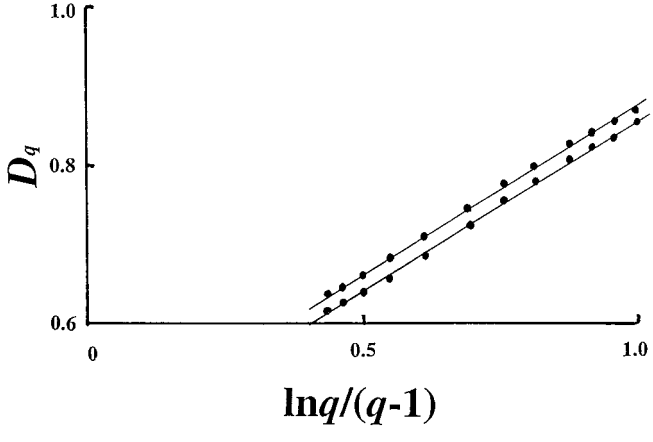

Fig. 7. Generalized dimensions D_q for a kicked rotator at two moments of the time (results of numerical simulation performed in ref. 11).

set of dots) and 6400 (upper set of dots). One can see that the multifractal Bernoulli representation (20) (straight lines) is in good agreement with these data as well.

6. DISCUSSION

Usually, known probability density functions are used to obtain relationships between moments of different orders (see, for instance, ref. 13). In the present paper we use a relationship between the moments, which appears at a morphological phase transition from monofractality to multifractality, to construct a new probability distribution (the multifractal Bernoulli distribution). Then, we compare this relationship with data obtained from numerical simulations performed by different authors for different critical mesoscopic systems to confirm that the multifractal Bernoulli distribution could be used to describe these systems.

It now seems to be an interesting problem for future investigations to calculate (numerically) the characteristic functions for the considered mesoscopic systems as well. Then one could compare these functions with the multifractal Bernoulli distribution (23) directly. It should be also noted a morphological origin of the new statistical distribution, so that morphological nature of the transitions in the critical mesoscopic systems seems to be an attractive subject both for analytical and for numerical investigations.

ACKNOWLEDGMENT

The author is grateful to a referee for comments and suggestion.

REFERENCES

1. M. Janssen, *Int. J. Mod. Phys. B* **8**:943 (1994).
2. B. L. Altshuler, V. E. Kravtsov, and I. V. Lerner, *Phys. Lett. A* **134**:488 (1989).
3. H. Aoki, *J. Phys. C* **16**:L205 (1983); *J. Phys. A* **134**:488 (1989).
4. S. Havlin and A. Bunde, *Physica D* **38**:184 (1989).
5. B. Huckstein and R. Klesse, *Phys. Rev. B* **55**:R7303 (1997).
6. M. Schreiber and H. Grussbach, *Phys. Rev. Lett.* **67**:607 (1991).
7. W. Pook and M. Janssen, *Z. Phys. B* **82**:295 (1991).
8. D. A. Parshin and H. R. Schrober, *Phys. Rev. B* **57**:10232 (1998).
9. B. Huckstein and L. Schweitzer, *Phys. Rev. Lett.* **72**:713 (1994).
10. I. Guaneri and M. Di Meo, *J. Phys. A* **28**:2717 (1995).
11. R. Artuso, D. Belluzzo, and G. Cassati, *Europhys. Lett.* **25**:181 (1994).
12. E. Parzen, *Modern Probability Theory and Its Applications* (Wiley, New York, 1967), Section 3.
13. A. Bershadskii, *Europhys. Lett.* **39**:587 (1997).

14. J. Beck and W. W. L. Chen, *Irregularities of Distribution* (Cambridge University Press, 1987), Section 1.
15. A. Bershadskii and A. Tsinober, *Phys. Lett. A* **165**:37 (1992).
16. H. E. Stanley and P. Meakin, *Nature* **335**:405 (1988).
17. L. D. Landau and E. M. Lifshitz, *Statistical Physics*, *Part 1* (Pergamon Press, 1980).
18. J. T. Chalker and P. D. Coddington, *J. Phys. C* **21**:2665 (1988).
19. R. Klesse and M. Metzler, *Europhys. Lett.* **32**:229 (1995).
20. J. T. Chalker and A. Dohmen, *Phys. Rev. Lett.* **75**:4496 (1995).
21. B. Bulka, M. Schreiber, and B. Kramer, *Z. Phys. B* **66**:21 (1987).
22. B. I. Shklovskii *et al.*, *Phys. Rev. B* **47**:11487 (1993).
23. P. W. Anderson, *Phys. Rev.* **109**:1492 (1958).
24. L. S. Levitov, *Europhys. Lett.* **9**:83 (1989).
25. V. L. Gurevich, D. A. Parshin, J. Pelous, and H. R. Schrober, *Phys. Rev. B* **48**:16318 (1993).
26. S. Fishman, D. R. Grempel, and R. E. Prange, *Phys. Rev. Lett.* **49**:509 (1982).